



Near-Field Effects in Mesoscopic Light Transport

R. Rezvani Naraghi,^{1,2} S. Sukhov,¹ J. J. Sáenz,^{3,4} and A. Dogariu^{1,*}

¹CREOL, The College of Optics & Photonics, University of Central Florida, Orlando, Florida 32816, USA

²Department of Physics, University of Central Florida, 4000 Central Florida Boulevard, Orlando, Florida 32816, USA

³Condensed Matter Physics Center (IFIMAC), Universidad Autónoma de Madrid, 28049 Madrid, Spain

⁴Donostia International Physics Center (DIPC), Paseo Manuel Lardizabal 4, 20018 Donostia-San Sebastian, Spain

(Received 10 August 2015; published 10 November 2015)

In dense multiple scattering media, optical fields evolve through both homogeneous and evanescent waves. New regimes of light transport emerge because of the near-field coupling between individual scattering centers at mesoscopic scales. We present a novel propagation model that is developed in terms of measurable far- and near-field scattering cross sections. Our quantitative description explains the increase of total transmission in dense scattering media and its accuracy is established through both full-scale numerical calculations and enhanced backscattering experiments.

DOI: 10.1103/PhysRevLett.115.203903

PACS numbers: 42.25.Dd, 42.68.Ay

Because of scattering in complex media, the phase, amplitude, and frequency of waves change randomly in time and space. The magnitude and direction of the power flux density changes continuously. Without accounting explicitly for wavelike manifestations (diffraction or interference), the energy transport is described as the conservation of so-called specific intensity [1]. When the radiation propagates over a distance ds along the direction s , the specific intensity reduces with $dI = -\rho(\sigma_{\text{sca}} + \sigma_{\text{abs}})I ds$ due to scattering and absorption but, at the same time, it also increases because of scattering with probability $P(s', s)$ from different directions s' into s . There are no practical solutions for this radiative transport depiction in most realistic situations. However, an angular moments expansion of the specific intensity leads to the ubiquitous description of diffusive transport [1]. This diffusion approximation is valid when the energy dissipation is minimal, the effective scattering is isotropic, and the source-detector separation is large compared to scattering length scales.

The diffusive energy transfer is characterized by different scales. Aside from absorption l_{abs} and scattering l_{sca} lengths, one also defines a transport mean-free path $l^* = l_{\text{sca}}/(1 - g)$ as the scale over which the isotropic diffusion establishes. The scattering asymmetry parameter g is defined [2] as the average of the cosine of the scattering angle $g \equiv \langle \cos \theta \rangle$. At this scale, the directional energy flux is randomized through successive scattering events. It is because of this randomization that details of particular interaction events are averaged out and simple energetic arguments provide an acceptable description of light propagation. A common representation of energy transport depicts the process as a classical random walk of particles of energy, photons [3]. The dynamic properties of this diffusion of photons can be described in terms of the scattering and dwell times involved and the associated velocities for phase, group, and energy transport [4,5].

Structural properties of random media determine different regimes of mesoscopic light transport. When the separation between scattering centers is much larger than the wavelength, the scattering events are considered to be independent. In this independent scattering approximation (ISA) the transport mean-free path $l_{\text{ISA}}^* = [n_0\sigma(1 - g)]^{-1}$ depends only on the number density n_0 of scattering centers, the optical cross section σ of an individual scatterer, and the asymmetry parameter g of a generic scattering event [2].

As the concentration of scatterers rises, the interparticle distances decrease and their spatial locations become correlated, leading to possible local interferences. The phase correlation between the scattered waves weakens the effective cross section below that of an individual scattering event. This collective scattering (CS) is quantified by the structure factor $S(q)$ determined by the pair-correlation function characterizing the spatial distribution of the scattering potential. In this case, the scattering phase function is renormalized $\tilde{P}(q) = P(q)S(q)$, which, in turn, modifies the effective scattering cross section $\sigma_{\text{CS}} = \int \tilde{P}(q)q dq$. The renormalization of the scattering process leads to a coherent correction $l_{\text{CS}}^* = [n_0\sigma_{\text{CS}}(1 - g_{\text{CS}})]^{-1}$ for the transport mean free path. The correlated particles can, therefore, be regarded as collections of pseudoscattering centers that are characterized by a modified scattering form factor [6,7]. In this interpretation, there is no further interaction between these fictitious scatterers. The interference between the scattered waves can increase the forward scattering and weaken the effective cross section below that of an individual scattering event $\sigma_{\text{CS}} < \sigma$. Positional correlations then lead to significantly large (wavelength dependent) transport mean free paths, which are responsible, for example, for the relatively large conductivity of disordered liquid metals [8,9] or the transparency of the cornea to visible light [10,11]. However, short-range order can also

lead to an enhanced effective cross section and negative values of the asymmetry parameter as it has been recently shown in experiments in colloidal liquids [12] and amorphous photonic materials [13,14]. The wavelength dependence of CS scattering is also the origin of natural structural coloration [15,16].

Multiple scattering effects are not considered within the CS description. As the particle density increases, the actual field incoming towards the scatterer includes not only the initial external field but also the fields scattered by the surrounding particles. In analogy with effective medium theories [17,18], different methods were proposed for homogenizing the environment, surrounding the location of a singular scattering event. A common approach is to use a modified form factor $P(q)$ corresponding to an isolated scatterer in a background with an effective refractive index n_{eff} and then use this information in conventional transport descriptions [13,16,19]. This refractive index homogenization eliminates the influence of the specific environment but a far-field description of scattering is still necessary.

At even higher densities, even this CS description fails [20,21] because, in close proximity, scattering centers can also interact through evanescent fields. This is clearly beyond the previous descriptions which not only consider the scatterers to act independently of their specific environment but also describe the scattering in terms of far-field properties such as Mie cross sections. Thus far, a precise, quantitative depiction of scattering for the case when the particles are located in the near field (NF) of each other is still missing even for the canonical example of spherical scatterers.

To set the limits for the conventional description of light transmission and to get quantitative insights into the physical situations typical to dense media, we first conducted systematic numerical calculations. Using a multiple sphere T -matrix approach [22], we evaluated rigorously the field distribution inside 3D composite media containing various distributions of particles. Typical results are shown in Figs. 1(a)–1(c) for the situation where particles in different concentrations are distributed throughout a cylindrical slab with different thicknesses L . More details about these calculations are included in the Supplemental Material [23]. It is readily observed in Fig. 1 that, as the concentration of particles increases, the mean interparticle distance decreases and more and more localized coupling occurs between neighboring particles.

In the classical description of diffusive transport through a slab of volume V and area A , the transmission scales according to Ohm's law: $T \propto l^*/L = V/N\sigma(1-g)L = A/N\sigma(1-g)$ [27]. This means that for a fixed ratio of area of the slab to number of particles A/N , the transmission is independent of the length of the medium. However, as apparent from the results of our simulations summarized in Fig. 1(d), the transmittance actually increases. This process

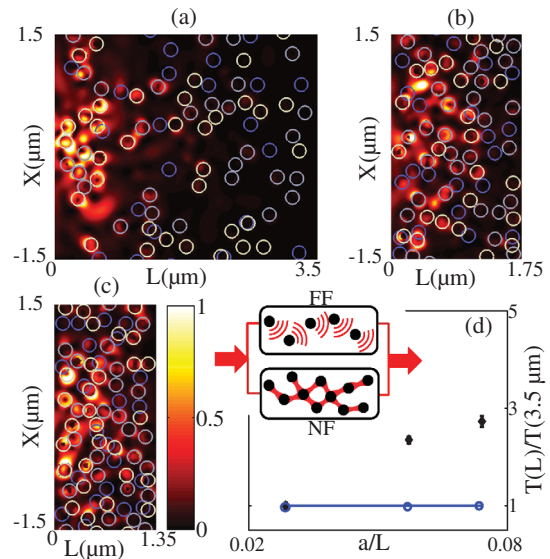


FIG. 1 (color). (a)–(c) Intensity distributions in the cross-sectional areas of 3D slabs with reducing lengths as indicated. The media contain $a = 100$ nm radius TiO_2 particles randomly dispersed throughout the volume. Rings colored in gray denote particles located in the considered cross section, while the white and blue ones indicate particles situated at 100 nm above and, respectively, below that plane. (d) Total transmission as a function of inverse thickness. The blue and black symbols designate the ISA and the results of T -matrix calculations, respectively. The inset illustrates the appearance of additional transmission channels due to near-field coupling (see text).

could be interpreted as a rise in the effective value of l^* or, alternatively, it can be described as the emergence of a different regime of mesoscopic transport.

When propagating in highly scattering media, optical waves comprise both homogeneous and inhomogeneous components. Thus, the energy is not only carried by propagating waves but it also evolves through evanescent coupling between individual scatterers. For linear random media, as scatterers become optically connected [20], near the onset of percolation, the near-field coupling between particles can be seen as an opening of new transmission, optically connected, channels as suggested in the inset of Fig. 1(d). High transmission through three-dimensional lattices of close packed spheres has been qualitatively explained as a percolation of light through overlapping whispering gallery modes [28]. In contrast with electronic systems, the appearance of optically connected channels is not expected to lead to percolation threshold phenomena [29]. Since power flows through both connected and scattering channels, the behavior of the transmittance should resemble that of thermal conductance of composites near percolation [30]: these new optically connected channels can be seen as adding parallel resistors to the (far-field) scattering channels [see inset in Fig. 1(d)]. As a result, the opening of these additional channels increases the overall transmission:

$$T = T_{\text{CS}} + T_{\text{NF}} = (l_{\text{CS}}^* + l_{\text{NF}}^*)L^{-1}. \quad (1)$$

In terms of discrete scattering processes, one can consider two types of events: (i) conventional Mie-like scattering where the illumination is provided by a plane wave and (ii) scattering events excited by evanescent waves. Of course, correcting the total transmission in this manner is practically relevant only if it can be described in terms of physically meaningful and measurable quantities such as a near-field scattering cross section σ_{NF} .

There were several notable attempts to calculate analytically or evaluate numerically the scattering of evanescent waves by spherical objects [31,32]. It has been shown that the conventional Mie theory can be directly applied to scattering of evanescent waves through a complex angle rotation of the standard Mie solution [33,34]. In this approach, by rotating both the direction and the distribution of the incident electric $\vec{E}(\vec{r}) = \hat{R}_y(-\gamma)\vec{E}[\hat{R}_y(\gamma)\vec{r}]$ and magnetic $\vec{H}(\vec{r}) = \hat{R}_y(-\gamma)\vec{H}[\hat{R}_y(\gamma)\vec{r}]$ fields by the complex angle γ , a z propagating monochromatic plane wave can be transformed into an evanescent wave. Thus, including this transformation in the conventional Mie calculation, one can readily find the results of the scattering of evanescent electromagnetic waves from spherical particles. We note that, due to the exponential decay of the evanescent wave, the scattering has some atypical features. In standard Mie scattering, because of the spherical symmetry, there are no cross-polarization terms in the scattering matrix. In the evanescent scattering, however, the exponentially decreasing amplitude introduces an asymmetry, which leads to such polarization mixing. Moreover, as opposed to standard theory, the Mie coefficients do not necessarily decrease with their order and the magnetic terms could actually be enhanced [31].

This demonstrates that σ_{NF} can be not only measured experimentally but it can also be easily evaluated numerically in the case of a spherical scatterer. Details about both calculations and measurements based on near-field scanning optical microscopy (NSOM), of near-field scattering are included in [23].

Grounded on the complete description of the scattering process including both homogeneous and inhomogeneous excitation, one can reinterpret the transport phenomena. Of course, particles can interact through evanescent waves only if they are in close proximity of each other. The process should therefore depend on both the number of scatterers per cubic wavelength $n_0\lambda^3$ and the strength of evanescent coupling determined by the average interparticle distance d [35], which, in turn, is set by the number density n_0 . The probability for evanescent transfer can then be written as $p_{\text{NF}} = n_0\lambda^3 e^{-\kappa d}$, where κ is the characteristic attenuation length for the evanescent waves. Thus, in the model where the light is transmitted through propagating and evanescent channels one can redefine the transport mean free path as

$$l_{\text{CS+NF}}^* = \frac{1}{n_0\sigma^*(1-g^*)} + \left(\frac{p_{\text{NF}}}{n_0\sigma_{\text{NF}}(1-g_{\text{NF}})} \right). \quad (2)$$

Because the decay rate of the evanescent waves depends on the incident angle, an average $\overline{(\dots)}$ is taken over the angular domain defined by the refractive indices of the particle and its surrounding medium. Moreover, as we mentioned before, the near-field cross section and the asymmetry parameter are both polarization dependent and, therefore, the values in Eq. (2) are also averaged over the two polarization states.

In practice, the complex angle rotation described before can be used to evaluate scattering properties such as scattering cross sections and asymmetry parameters. These values can then be used in Eq. (2) to evaluate the transport mean free path for media with different particle concentrations. It is worth mentioning here that l^* is the only directly measurable quantity in a multiple-scattering experiment such as, for instance, enhanced backscattering (EBS).

To verify the accuracy of our model, we conducted an EBS experiment on colloidal media with increasing concentrations. We used aqueous suspensions silica particles with an average diameter of 1 μm . The schematic representation of the experimental setup is shown in Fig. 2(a). A collimated laser beam with $\lambda = 476$ nm passes through a beam splitter and through a filter consisting of a linear polarizer followed by a quarter wave plate. The circular-polarization filter ensures that no single-scattering contributions are collected. The circularly polarized beam further impinges on a glass cuvette containing colloidal suspension. The backscattered light is deflected by the beam splitter and then is focused by a lens with 250 mm focal length on the plane of a CCD array (520 \times 480 pixel array). During the measurements, an ensemble average is performed by recording typically 100 different data frames. Details about EBS measurements are included in [23].

The results corresponding to different colloidal concentrations are summarized in Fig. 2(b) where the experimental l^* values are normalized to the corresponding ones evaluated in the ISA framework. As can be seen, when increasing the concentration of the particles, the measured transport mean free path starts to deviate from both the ISA predictions and the estimations based on the CS correction model. On the other hand, our near-field transmission model shows a remarkably good agreement with the experimental data. The remaining minor differences may be attributed to experimental conditions such as internal reflection [25,26] and potential sample nonuniformities [36,37]. We note that this experimental demonstration augments the significance of our previous numerical calculations: the increase of l^* values due to additional near-field

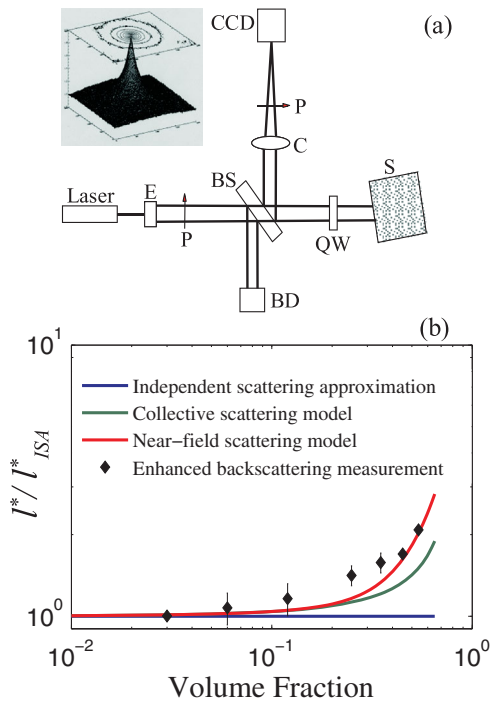


FIG. 2 (color). (a) Enhanced backscattering setup. Abbreviations are as follows: *E*, beam expander; *P*, polarizers; BS, beam splitter; BD, beam detector; QW, quarter-wave plate; *C*, Fourier lens; *S*, sample. (b) Measured transport mean free path compared with predictions of different transport models.

coupling is apparent in both transmission and reflection. At high volume fractions, both experimental and numerical data clearly illustrate the failure of the conventional description of scattering solely in terms of propagating waves.

In conclusion, we have quantitatively described the characteristics of multiple light scattering in dense composite media where particles are located in close proximity and interact through evanescent near-fields. We have shown that a new regime of transmission emerges, which can be described in terms of physically meaningful and measurable quantities such as a near-field scattering cross section σ_{NF} . In this regime, additional transmission channels open because of the near-field interactions between scatterers placed in close proximity.

A full-scale calculation of the electromagnetic field distribution in 3D random media indicates the emergence of additional channels for energy transfer. The model is also supported by the results of a comprehensive EBS experiment. We found that the transport mean free path corresponding to the different concentration of scatterers is in very good agreement with our model for near-field corrected transport. The use of such detailed descriptors for individual scattering events not only improves the macroscopic description of light propagation in random media but it also enhances the predictive capabilities of light transport models.

The computing time provided by STOKES ARCC at the University of Central Florida (UCF) is gratefully acknowledged. This work was partially supported by the Air Force Office of Scientific Research (Grant No. FA95501010190). J. J. S. was supported by the Spanish Ministry of Economy and Competitiveness (Grant No. FIS2012-36113-C03).

*Corresponding author.

adogariu@creol.ucf.edu

- [1] A. Ishimaru, *Wave Propagation and Scattering in Random Media* (Academic Press, Inc., New York, 1978).
- [2] C. F. Bohren and D. R. Huffman, *Absorption and Scattering of Light by Small Particles* (John Wiley & Sons, New York, 2008).
- [3] A. H. Gandjbakhche and G. H. Weiss, *Prog. Opt.* **34**, 333 (1995).
- [4] E. P. Wigner, *Phys. Rev.* **98**, 145 (1955).
- [5] G. Cwilich and Y. Fu, *Phys. Rev. B* **46**, 12015 (1992).
- [6] P. M. Saulnier, M. P. Zinkin, and G. H. Watson, *Phys. Rev. B* **42**, 2621 (1990).
- [7] S. Fraden and G. Maret, *Phys. Rev. Lett.* **65**, 512 (1990).
- [8] J. M. Ziman and *Philos. Mag. B* **6**, 1013 (1961).
- [9] N. W. Ashcroft and J. Lekner, *Phys. Rev.* **145**, 83 (1966).
- [10] R. W. Hartand and R. A. Farrell, *J. Opt. Soc. Am.* **59**, 766 (1969).
- [11] G. B. Benedek, *Appl. Opt.* **10**, 459 (1971).
- [12] L. F. Rojas-Ochoa, J. M. Mendez-Alcaraz, J. J. Sáenz, P. Schurtenberger, and F. Scheffold, *Phys. Rev. Lett.* **93**, 073903 (2004).
- [13] M. Reufer, L. F. Rojas-Ochoa, S. Eiden, J. J. Sáenz, and F. Scheffold, *Appl. Phys. Lett.* **91**, 171904 (2007).
- [14] P. D. García, R. Sapienza, A. Blanco, and C. López, *Adv. Mater.* **19**, 2597 (2007).
- [15] R. O. Prum, R. H. Torres, S. Williamson, and J. Dyck, *Nature (London)* **396**, 28 (1998).
- [16] S. F. Liew, J. Forster, H. Noh, C. F. Schreck, V. Saranathan, X. Lu, L. Yang, Richard O. Prum, C. S. O'Hern, E. R. Dufresne, and H. Cao, *Opt. Express* **19**, 8208 (2011).
- [17] P. Sheng, *Phys. Rev. Lett.* **45**, 60 (1980).
- [18] K. Busch and C. M. Soukoulis, *Phys. Rev. Lett.* **75**, 3442 (1995).
- [19] X. T. Peng and A. D. Dinsmore, *Phys. Rev. Lett.* **99**, 143902 (2007).
- [20] R. Sapienza, P. D. Garcia, J. Bertolotti, M. D. Martin, A. Blanco, L. Vina, C. Lopez, and D. S. Wiersma, *Phys. Rev. Lett.* **99**, 233902 (2007).
- [21] P. D. Garcia, R. Sapienza, J. Bertolotti, M. D. Martin, A. Blanco, A. Altube, L. Vina, D. S. Wiersma, and C. López, *Phys. Rev. A* **78**, 023823 (2008).
- [22] D. W. Mackowski and M. I. Mishchenko, *Phys. Rev. A*, **83**, 013804 (2011).
- [23] See Supplemental Material at <http://link.aps.org/supplemental/10.1103/PhysRevLett.115.203903> for details on calculations and NSOM measurements of the near-field phase function, numerical calculation for transmission, and enhanced backscattering measurements, which includes Refs. [22,24–26].

- [24] E. Akkermans, P. E. Wolf, R. Maynard, and G. Maret, *J. Phys. (Paris)* **49**, 77 (1988).
- [25] J. X. Zhu, D. J. Pine, and D. A. Weitz, *Phys. Rev. A* **44**, 3948 (1991).
- [26] G. Popescu, C. Mujat, and A. Dogariu, *Phys. Rev. E* **61**, 4523 (2000).
- [27] E. Akkermans and G. Montambaux, *Mesoscopic Physics of Electrons and Photons* (Cambridge Univ. Press, Cambridge, 2007).
- [28] V. N. Astratov and S. P. Ashili, *Opt. Express* **15**, 17351 (2007).
- [29] S. Kirkpatrick, *Rev. Mod. Phys.* **45**, 574 (1973).
- [30] Y. P. Mamunya, V. V. Davydenko, P. Pissis, and E. V. Lebedev, *Eur. Polym. J.* **38**, 1887 (2002).
- [31] C. Herman, D. Wang, and M. Kerker, *Appl. Opt.* **18**, 2679 (1979).
- [32] C. Liu, T. Kaiser, S. Lange, and G. Schweiger, *Opt. Commun.* **117**, 521 (1995).
- [33] D. Barchiesi and D. Van Labeke, *J. Mod. Opt.* **40**, 1239 (1993).
- [34] A. Y. Bekshaev, K. Y. Bliokh, and F. Nori, *Opt. Express* **21**, 7082 (2013).
- [35] S. Torquato, *Phys. Rev. E* **51**, 3170 (1995).
- [36] P. N. Pusey and W. van Megen, *Phys. Rev. Lett.* **59**, 2083 (1987).
- [37] N. M. Dixit and C. F. Zukoski, *Phys. Rev. E* **64**, 041604 (2001).